



Scholars Research Library

Der Pharma Chemica, 2011, 3 (6):41-52
(<http://derpharmachemica.com/archive.html>)



ISSN 0975-413X
CODEN (USA): PCHHAX

Growth, Structural, Vibrational, Mechanical, and Dielectric Studies of KSb_2F_7 Crystals

¹C. Besky Job, ¹K. Ganesan, and ²J. Benet Charles.

¹Department of Physics, M.S. University, Tirunelveli, India

²Materials Research Centre, Department of Physics, St. Xavier's College, Palayamkottai, India

ABSTRACT

The interest in Fluoro Antimonate crystals have been increased in the last four decades due to its superionic conduction and its unusual electro optic properties. Potassium hepta fluoro di antimonate (KSb_2F_7) crystals has been grown by slow evaporation technique. KSb_2F_7 crystal crystallizes into monoclinic structure with space group $P2_1/C$. The functional groups present in the crystal were determined using FTIR spectroscopy. The microhardness study shows that hardness steadily increases, then decreases for higher loads. Work hardening coefficient indicates that the grown crystals are moderately softer. The variation of dielectric constant, dielectric loss, and A.C. conductivity with temperature at different frequencies were discussed. It was found that both the dielectric constant and dielectric loss decrease with increase in frequency.

Key words : X-ray diffraction, Micro hardness, Dielectric Constant, A.C. Conductivity.

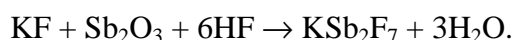
INTRODUCTION

Many compounds of complex antimony (III) fluorides have anomalous electro physical, optical and other properties (1-3). Many publications are devoted to investigation on the structure and properties of MSb_2F_7 crystals (M = sodium, potassium, cesium, rubidium , ammonium, and thallium). The structures of KSb_2F_7 [4], RbSb_2F_7 [5], CsSb_2F_7 [6], TlSb_2F_7 [7] and NaSb_2F_7 [8] were determined. Anomalously high ionic conduction was observed in the temperature range 400-480 K : $\sigma \approx 10^{-2}$ - 10^{-4} Ohm /cm in complex antimony (III) fluorides such as TlSb_2F_7 [9], $\text{NH}_4\text{Sb}_2\text{F}_7$ [9,10] and KSb_2F_7 [11]. KSb_2F_7 , one of the important Antimony Fluoride Compound (AFC) has the greatest activating effect to stimulate the photosynthesis in U. fenestrata alga [12]. The structure of KSb_2F_7 consists of polymeric chains formed by alternating octahedral $\text{Sb}(1)\text{F}_5\text{E}$ (E is un shared electron pair of Sb^{3+}) and trigonal bipyramids $\text{Sb}(2)\text{F}_4\text{E}$ linked by asymmetric fluoride bridges [12]. No attempt has been made on micro hardness and dielectric studies of KSb_2F_7 crystals. In the present investigation, we report the growth, powder and single crystal XRD techniques along with FTIR, micro hardness and dielectric studies of KSb_2F_7 crystals.

MATERIALS AND METHODS

2.1 Crystal growth

KSb₂F₇ was synthesized by dissolving the appropriate amount of KF, Sb₂O₃ and HF in double-distilled water and stirred well at 303K to form homogeneous solution. The chemical reaction is



The saturated solution was purified further by repeated recrystallization and allowed to evaporate the excess amount of water at 303K to obtain seed crystals due to spontaneous nucleation within a week. The single crystals of KSb₂F₇ were successfully grown from aqueous solution by slow evaporation technique in a period of two weeks. The grown crystals were shown in Fig. 1.

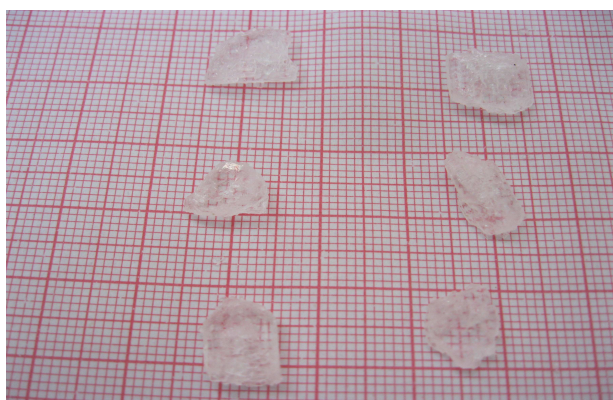


Fig. 1. The grown KSb₂F₇ crystal

2.2 Material Characterization

Powder X-ray diffraction technique has been used to investigate the crystal structure of the grown crystal (Philips X'pert Pro X-ray Automatic diffractometer). The single crystal X-ray diffraction has been carried out using ENRAF NONIUS CAD4 diffractometer with MoK α radiation ($\lambda=0.7107 \text{ \AA}$). Infra red spectroscopy has been utilized to identify the functional groups of the synthesized compounds. The FTIR spectrum has been recorded in the range of 400 – 4000 cm^{-1} by KBr pellet technique using 8400S Shimadzu FTIR Spectrometer. The mechanical property of the grown crystals has been studied using a Reichert MD 4000E Vickers ultra micro hardness tester attached to metallurgical optical microscope. A well polished KSb₂F₇ crystal was placed on the platform of Vickers micro hardness tester and the loads of different magnitudes were applied over a fixed interval of time. The indentation time was kept 10 sec for all loads. The diagonal length of each indentation has been recorded and the average of the diagonal lengths has been computed. For dielectric studies, flat polished surfaces of the crystal were coated with silver paint and is inserted in between the sample holders. The dielectric constant(ϵ_r), dielectric loss ($\tan\delta$) and A.C. conductivity (σ_{ac}) were obtained as a function of frequency (100Hz – 1MHz) at different temperatures (273K to 423K) using Agilent 4284 A 20Hz-1MHz precision LCR meter.

RESULTS AND DISCUSSION

3.1 XRD analysis

Figure 2 shows the standard and indexed XRD pattern of the grown KSb₂F₇ crystal. The pattern has been indexed with the JCPDS file 71 – 1945 as shown in the figure which confirms the presence of KSb₂F₇ crystal structure. This result has also been reported by S.H. Mastin *et al* [4].

The crystal exhibits monoclinic system with space group $P2_1/C$. The cell parameters were measured as $a = 10.51 \text{ \AA}$, $b = 7.598 \text{ \AA}$, $c = 8.601 \text{ \AA}$ and $\beta = 100.82^\circ$. The calculated volume of the unit cell is 674.7 \AA^3 . The lattice parameters are in good agreement with those values already reported thus confirming the grown crystal [4].

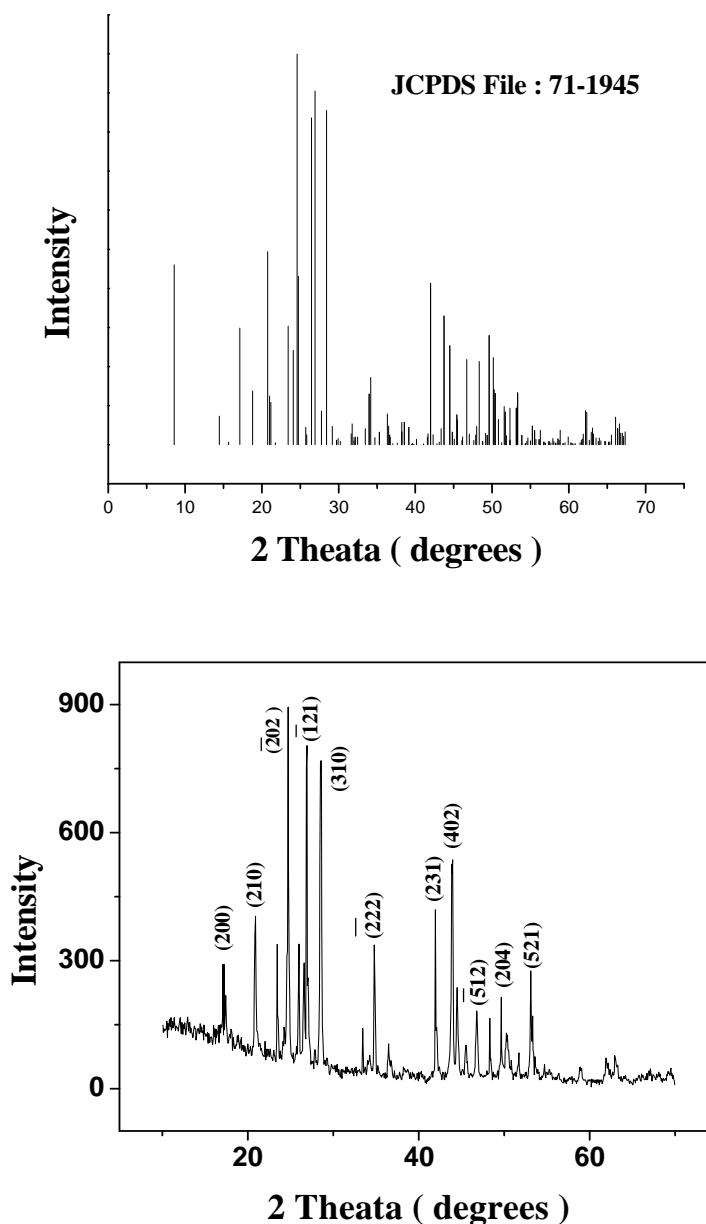


Fig. 2. Standard and indexed Powder XRD pattern of KSb_2F_7 crystal

3.2. FTIR analysis

The recorded FTIR spectrum of KSb_2F_7 is depicted in Fig. 3. The stretching vibrations of H_2O are characterized by an intense absorption band with maxima at 3529 cm^{-1} indicates that these compounds contain small quantity of water [13]. The deformation vibration of H_2O gives a medium intensity band at 1717 cm^{-1} [14]. A narrow band with the minimum at 1224 and 1367 cm^{-1} corresponding to the bending vibrations of Sb-O-Sb bond [15]. An intense band at 754 cm^{-1} in the IR spectrum is responsible for asymmetric stretching vibrations of Sb-O-Sb bond [16]. It is assigned that the intense line at 518 cm^{-1} corresponds to the symmetric stretching vibrations of

Sb-F bonds. ($\nu_1 A_1$) [13,17,18]. We think that the weak line at 1059cm^{-1} does not belong to the principal vibrations of antimony (III) fluoride complexes.

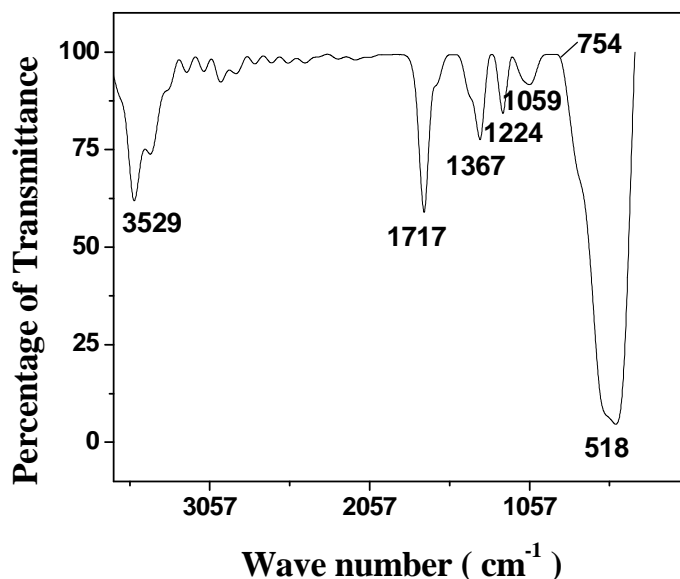


Fig. 3. FTIR spectrum of K Sb₂ F₇ crystal

3.3 Microhardness studies

3.3.1 Variation of hardness with load

The Vicker's hardness value (H_v) has been calculated from the formula,

$$H_v = 1.8544 P/d^2 \text{ Kgmm}^{-2}$$

where P represents load, d is the diagonal length of the indentation impression [19]. A plot has been drawn between hardness number (H_v) and applied load (P) is as shown in Fig. 4.

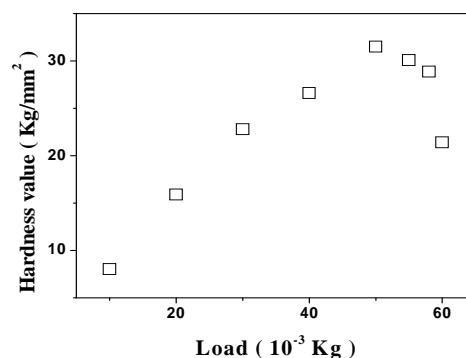


Fig. 4. Variation of hardness with load for K Sb₂ F₇ crystal

In the present study, hardness value increases to a maximum up to a load of 50gm, and thereafter decreases for higher loads. According to Sangwal [20] in the initial stage (i.e. at low loads or strains) plastic deformation of crystals mainly involves the nucleation of dislocations along a particular slip system. When only one slip system is active during plastic deformation, at low loads the number of active parallel glide planes during indentation is low. Therefore the nucleating dislocations rapidly propagate into the material without experiencing substantial stress

between them. Consequently in this stage indentation depth h increases proportionally with indentation pressure. However, with increasing load when the number of parallel glide plane increases, the motion of dislocations gliding in them is slowed down due to the mutual interaction stress between dislocation. This leads to a slow indentation depth h with increasing indentation pressure. Consequently, the increase in H_v with h steadily becomes weaker until H_v attains a steady value after some particular value of load.

3.3.2 Log P vs log d plot

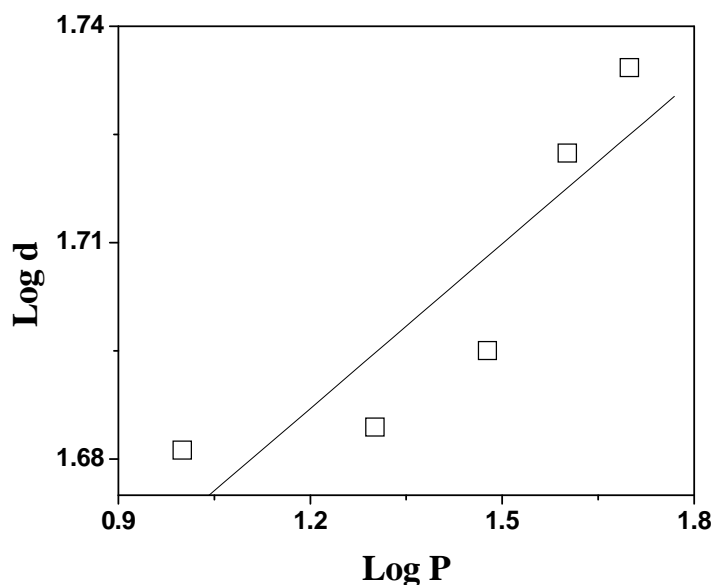


Fig. 5. Plot of log p versus log d for KSb_2F_7 crystal

The relation between the load and size of the indentation is given by

$$P = k_1 d^n \quad (1)$$

where P is the load, d is the diagonal length of impression, n is the work hardening coefficient, a measure of the strength of the crystal, is computed from the log p -log d plot (Fig. 5). K_1 is the standard hardness found out from the intercept. From careful observations on various materials, Onitsch [21] pointed out that n lies between 1 and 1.6 for hard materials and it is more than 1.6 for soft materials. The value of n observed in the present study is 1.6 suggesting that KSb_2F_7 crystal is a moderately softer substance. n value for $\text{NH}_4\text{Sb}_2\text{F}_7$ is 2.3. [22] and NaSb_2F_7 is 1.36 [23]. It indicates that when different substances such as sodium and ammonium added with heptafluorodiantimonate, its n value changes enormously.

3.3.3 d vs $d^{n/2}$ plot :

It is known that the material takes some time to revert to elastic mode after the applied load is removed. So a correction factor x is applied to the d value.

$$P = k_2 (d+x)^2 \quad (2)$$

Sub eqn (1) in eqn (2)

$$K_1 d^n = k_2 (d+x)^2 \quad (3)$$

Simplifying

$$d^{n/2} = (k_2/k_1)^{1/2} d + (k_2/k_1)^{1/2} x \quad (4)$$

The slope of $d^{n/2}$ vs d yields $(k_2/k_1)^{1/2}$ and the intercept is a measure of x . (Fig.6).

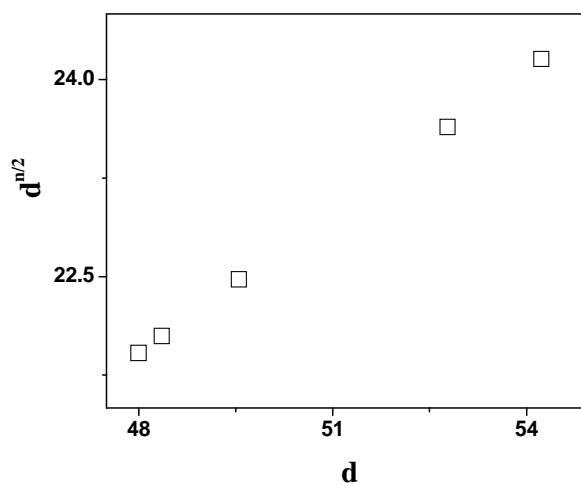


Fig. 6. Plot of d vs $d^{n/2}$ for KSb_2F_7 crystal

3.3.4 Yield strength

From the hardness value, the yield strength (σ_y) can be calculated using the relation,

$$\sigma_y = H_v / 2.9 \{ [1 - (2-n)] [(12.5(2-n) / 1 - (2-n))^{2-n}] \}$$

The yield strength is calculated to be 1.822 Mpa. The hardness parameters are listed in Table 1.

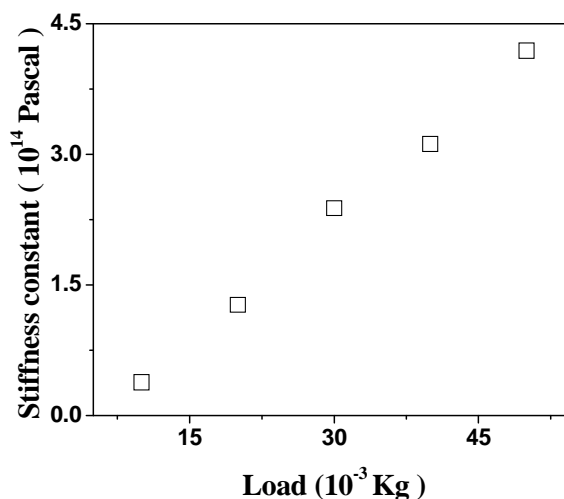


Fig. 7. Variation of stiffness constant with load for KSb_2F_7 crystal

Table 1. Hardness parameters of KSb_2F_7 crystal

n	k_1 (10 ⁻³ Kg)	k_2 (10 ⁻³ Kg)	x (μm)
1.521	1.1336	31.6544	0.049

3.3.5 Variation of stiffness constant with load

The elastic stiffness constant (C_{11}) gives an idea about the tightness of bonding between neighbouring atoms. The stiffness constant for different loads has been calculated using wooster's empirical formula. $C_{11}=(Hv)^{7/4}$ [24]. From the graph (Fig. 7) it is clear that the stiffness constant increases with increase of load. High value of C_{11} indicates that the binding forces between the ions are quite strong [25].

3.4 Dielectric and A.C. Conductivity Studies

The variation of dielectric constant (ϵ_r) against frequency for KSb_2F_7 crystals along a, b, and c, directions are shown in Fig. 8, 9, 10. The dielectric constant was evaluated by using the following equation.

$$\epsilon_r = \frac{\left[\left(C_{\text{crys}} - C_{\text{air}} \right) \left(\frac{1 - A_{\text{crys}}}{A_{\text{air}}} \right) \right] A_{\text{air}}}{C_{\text{air}} A_{\text{crys}}}$$

where C_{crys} is the capacitance of the crystal. C_{air} is the capacitance of the air of the same dimension as the crystal, A_{crys} and A_{air} are the area of the crystal and area of the electrode respectively [26].

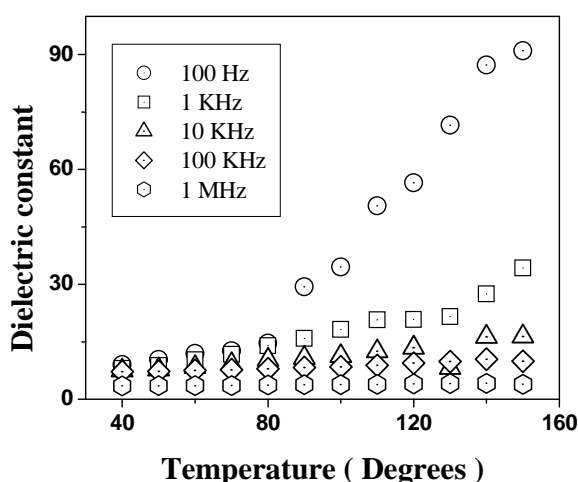


Fig. 8. Variation of Dielectric constant with temperature at different frequencies in 'a' axis for KSb_2F_7 crystal

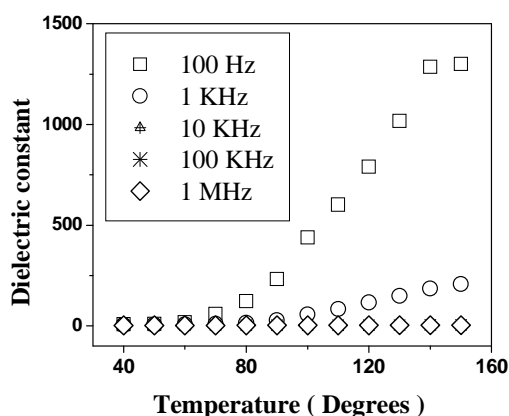


Fig. 9. Variation of Dielectric constant with temperature at different frequencies in 'b' axis for KSb_2F_7 crystal

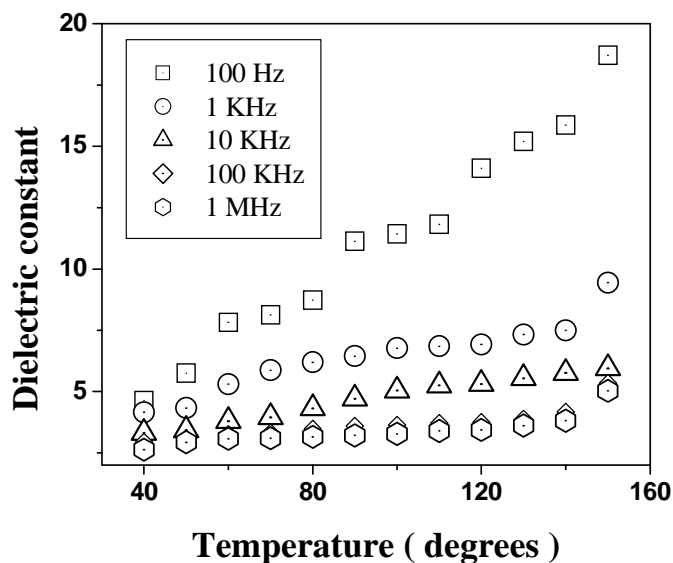


Fig. 10. Variation of Dielectric constant with temperature at different frequencies in 'c' axis for KSb_2F_7 crystal

The different values of dielectric constant in different directions confirms the anisotropy of the given crystal used in the present study.

The dielectric behaviour in the first interval is observed in the low frequency region 100Hz – 10KHz in which ϵ' sharply decreases with increasing frequency. This may be due to the contribution of space charge polarization. The space charge polarization will depend on the purity and perfection of the material. [27].

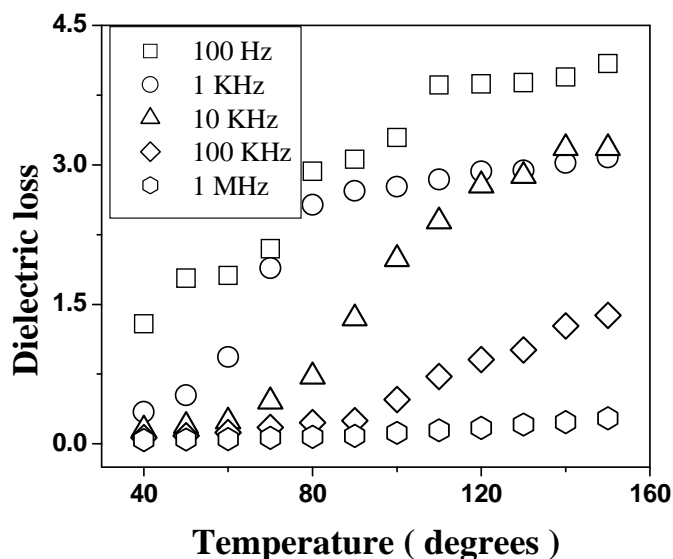


Fig. 11. Variation of Dielectric loss with temperature at different frequencies in 'a' axis for KSb_2F_7 crystal

Dielectric behaviour in the second interval is observed in the high frequency region 100KHz – 1 MHz, in which ϵ' decreases slightly with increasing frequency. As the frequency increases, a point will be reached where the space charge cannot sustained and comply with the external field giving rise to diminishing values of dielectric constant. The dielectric constant is observed to increase with temperature due to the orientation of dipoles which facilitate the increase in

permittivity at higher temperature [28] The variation of dissipation factor ($\tan \delta$) with temperature at different frequencies of the applied a.c. field in a, b, c directions are shown in figures 11,12, 13,

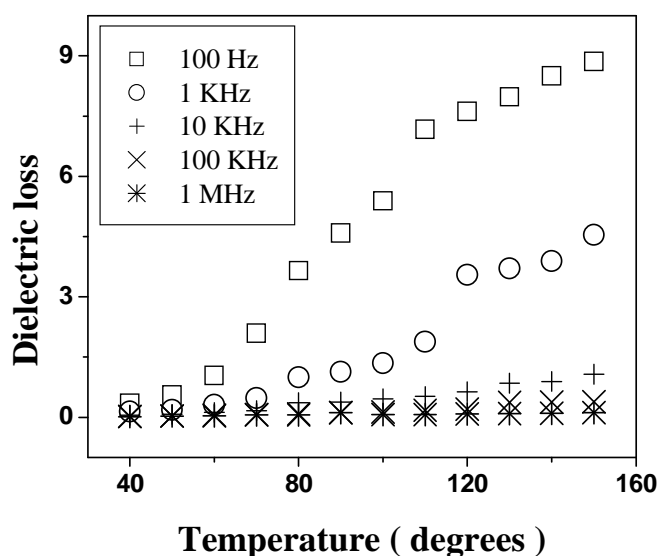


Fig. 12. Variation of Dielectric loss with temperature at different frequencies in 'b' axis for KSb_2F_7 crystal

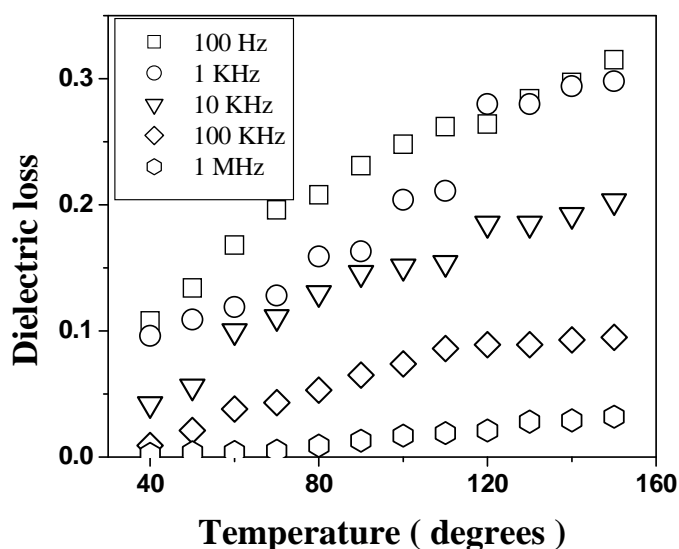


Fig. 13. Variation of Dielectric loss with temperature at different frequencies in 'c' axis for KSb_2F_7 crystal

Low values of $\tan \delta$ suggests that the grown crystals are of moderately good quality. Figures 14,15, 16 illustrates the temperature dependence of A.C. conductivity at different frequencies in a, b, c directions. A.C. conductivity is noted to be slightly increased with increasing temperature in the low temperature region. It fulfills an intensive rise with increasing temperature in high temperature region is mainly attributed to the thermally generated charge carriers [29]

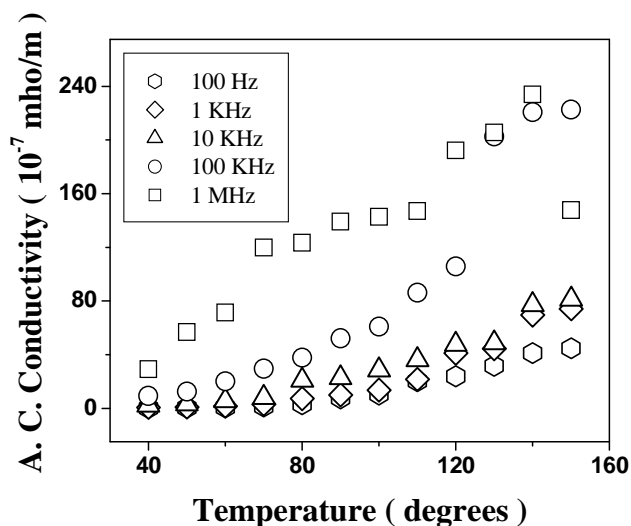


Fig. 14. Variation of A.C. Conductivity with temperature at different frequencies in 'a' axis for KSb_2F_7 crystal

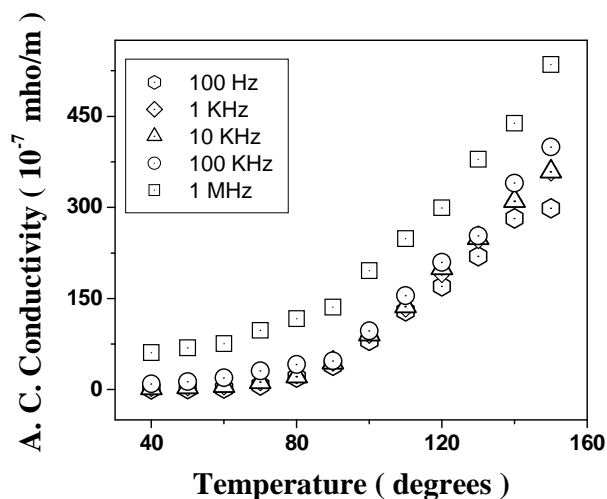


Fig. 15. Variation of A.C. Conductivity with temperature at different frequencies in 'b' axis for KSb_2F_7 crystal

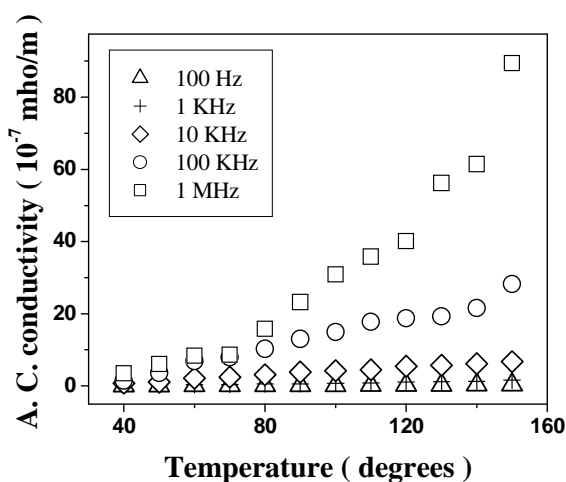


Fig. 16. Variation of A.C. Conductivity with temperature at different frequencies in 'c' axis for KSb_2F_7 crystal

CONCLUSION

Good quality single crystals of KSb_2F_7 were grown within a period of two weeks by slow evaporation method. KSb_2F_7 compound crystallizes into monoclinic structure with space group $\text{P2}_1/\text{C}$. The FTIR spectral analysis reveals the presence of functional groups of the crystal. Micro hardness test showed that these crystals belongs to moderately softer category. The Yield Strength of the crystal used in the present study is 1.822 MPa. Dielectric constant and dielectric loss decrease with increasing frequency.

REFERENCES

- [1] R.L. Davidovich, P.S. Gordienko, J. Grigas, *Phys. Stat. Solidi (a)*, **1984**, 84, 387.
- [2] M.P. Borzenkova, F.V. Kalinchenko, A.V. Novoselova, *Rus. J. Inorg. Chem.*, **1984**, 29, 703.
- [3] J.G. Bergman, D.S. Chemla, R. Fourcade, G. Mascherpa, *J. Solid State Commun.*, **1978**, 3, 187.
- [4] S.H. Mastin and R.R. Ryan, *Inorg. Chem.*, **1971**, 10, 1757.
- [5] D. Tichit, B. Ducourant, R. Fourcade, G. Mascherpa, *J. Fluor. Chem.*, **1979**, 13, 45.
- [6] R.R. Ryan, S.H. Mastin and A.C. Larson, *Inorg. Chem.*, **1971**, 10, 2793.
- [7] A.A. Udovenko, Yu. E. Gorbunova, R.L. Davidovich, *Rus. J. Coord. Chem.*, **2000**, 26, 662.
- [8] J. Benet Charles, F.D. Gnanam, *Mat. Chem and Phy.*, **1994**, 38, 337.
- [9] V.Ya. Kavun, N.F. Uvarov, L.A. Zemnukhova, A.B. Slobodyuk, *J. Struct. Chem.*, **2002**, 43, 766.
- [10] V.Ya. Kavun, V.I. Sergienko, N.I. Sorokin, L.A. Zemnukhova, T.A. Kaidalova and E.B. Merkulov, *J. Struct. Chem.*, **2001**, 42, 570.
- [11] V.ya. Kavun, N.F. Uvarov, A.B. Slobodyuk, O.V. Brovkina, L.A. Zemnukhova V.I. Sergienko, *Rus. J. Electro Chem.*, **2005**, 41, 488.
- [12] E.V. Kovaleva, L.A. Zemnukhova, V.H. Nikitin, M.D. Koryakova N.V. Speshneva, *Rus. J. App. Chem.*, **2002**, 75, 954.
- [13] L.A. Zemnukhova, R.L. Davidovich, A.A. Udovenko E.V. Kovaleva, *Rus. J. Coord. Chem.*, **2005**, 31, 115.
- [14] N. M. Laptash, E. V. Kovaleva, A. A. Mashkovskii, A. Yu. Beioliptsev, L. A. Zemnukhova, *J. Struct. Chem.*, **2007**, 48, 848.
- [15] T.G. Balicheva, N.I. Roi, *Rus. J. Inorg. Chem.*, **1972**, 17, 1556.
- [16] E.I. Voit, A.E. Panasenko, L.A. Zemnukhova, *J. Struct. Chem.*, **2009**, 50,60.
- [17] Kazuo Nakamoto , *Infrared and Raman spectra of Inorganic and Coordination Compounds*, John Wiley & Sons, Newyork, **1986**.
- [18] V.V. Fomichev, K.I. Petrov, L.A. Sadokhina, *Rus. J. Inorg. Chem.*, **1972**, 17, 1348.
- [19] B.W. Mott, *Microindentation Hardness Testing*, Butterworths, London, **1956**
- [20] K. Sangwal, *Mat. Chem. and Phy.*, **2000**, 63, 145.
- [21] E.M. Onistch, *Mikroskopie*, **1947**, 2, 131.
- [22] R. Christhu Dhas, J. Benet Charles, F.D. Gnanam, *J. Mat.Sci. Lett.*, **1993**, 12 1395.
- [23] J. Benet Charles, F.D. Gnanam, *J. Mat. Sci. Lett.*, **1990**, 9, 165.
- [24] W. A. Wooster, *Rep. Progr. Phys.*, **1953**, 16, 62
- [25] R. Ashok kumar, R. Ezhil Vizhi, N. Vijayan, D. Rajan Babu, *Der Pharma Chemica.*, **2010**, 2, 247.
- [26] M. Meena, C.K. Mahadevan, *Crys. Res. Tech.*, **2008**, 43, 166.
- [27] A. Cyrac Peter, M. Vimalan, P. Sagayaraj, J. Madhavan, *Der Pharma Chemica.*, **2010**, 2, 191.

[28] Poonam Sharma, D. K. Kanchan, Meenakshi Pant, K. Padmasree, *Ind. J. Pure and App. Phys.*, **2010**, 48, 39.

[29] A. J. Jeyaprakash Manoharan, N. Joseph John, V. Revathi, K. V. Rajendran, P. M. Andavan, *Ind. J. Sci. and Tech.*, **2011**,4, 688.